

Energy-Efficient Power Adaptation over a Frequency-Selective Fading Channel with Delay and Power Constraints

Amir Helmy, *Student Member, IEEE*, Leila Musavian, *Member, IEEE*, and Tho Le-Ngoc, *Fellow, IEEE*

Abstract—This paper presents an energy-efficient power allocation for a multicarrier link over a frequency-selective fading channel with a delay-outage probability constraint. The power adaptation maximizes the system energy efficiency (EE), formulated as the ratio of the achieved effective capacity (EC) to the total expenditure power, including both transmission power and rate-independent circuit power. We prove that this objective function is quasi-concave in the transmission power, and derive the global optimum solution using fractional programming. Based on the obtained solution, we develop a power adaptation algorithm consisting of two steps: (i) establishing the optimum average power level corresponding to the maximum achievable EE with no transmit power constraint, and then (ii) for a given power constraint, jointly distributing the power over time and frequency based on the constraint and the optimum power level found in the first step. Analytical results show that the proposed EE-based power allocation has a structure similar to the allocation that maximizes the EC, but with a different cut-off threshold. Our proposed joint EE-optimal power allocation provides significant EE gains over both the joint spectral-efficient and independent-subcarrier EE-based power allocation schemes, where the rate-energy tradeoff becomes more pronounced with higher frequency selectivity.

Index Terms—Multicarrier system, quality-of-service (QoS), delay-outage probability constraint, effective capacity (EC), energy efficiency (EE), fractional programming.

I. INTRODUCTION

NEXT-GENERATION wireless networks, including the fourth-generation (4G) cellular systems, are expected to support diverse quality-of-service (QoS) requirements since different services demand different levels of QoS guarantees [1]. For example, in real-time multimedia services such as video transmission, if a received packet violates its delay limit then it is considered useless and must be discarded. Consequently, mechanisms for guaranteeing QoS, such as resource allocation and admission control, need to be developed in

an efficient manner. To facilitate the design of QoS-support communication systems, queuing analysis is required whereby the source traffic and the channel service are matched using a first-in-first-out (FIFO) buffer. This buffer allows the modeling of wireless channels in terms of QoS metrics such as data rate, delay, and QoS violation probability. In particular, effective capacity (EC) is proposed in [2] as a QoS-aware metric that specifies the maximum constant arrival rate that a system can support while satisfying a target delay requirement indicated by a QoS exponent.

The problem for maximizing the EC of a multicarrier system with frequency-selective fading channel is studied in [3]. It was shown that maximizing the EC at each subchannel independently, using the optimal power adaptation policy for single-channel flat-fading channels obtained in [4], does not yield an optimal scheme. Hence, using the framework of joint convex optimization, the authors in [3] propose an optimal QoS-driven spectral-efficient power allocation under an average transmit power constraint. The analysis shows that when the QoS exponent increases from zero to infinity, the optimal EC decreases accordingly from the ergodic capacity to zero-outage capacity.

Exponentially increasing data traffic comes at the cost of rapidly increasing energy consumption, which is sometimes unaffordable for energy-limited systems. Consequently, energy-efficient system design has recently received growing attention by many research groups. Energy efficiency (EE) is defined as the data transferred per unit energy consumed with units of bits per joule (b/J), or equivalently, the ratio of the achieved rate to the total power expenditure. The trade-off between EE and spectral efficiency (SE) has been investigated in [5], whereby Shannon capacity is considered as a measure of the service rate and the power consumption does not account for the circuit power. In [6]–[10], the total dissipated power is considered to have two components: circuit power in addition to a transmission power. The EE curve as a function of the transmit power was shown in [6] to have a bell shape where the location of its maximum depends on the circuit power. Under assumption of perfect channel state information (CSI) at receiver, energy-efficient power adaptation schemes were developed in [10] and [11] for point-to-point flat-fading channels without and with transmit CSI, respectively. Optimal power and subchannel allocation schemes are proposed in [7] to maximize the EE of a wireless orthogonal frequency division multiple access (OFDMA) system with flat-fading

Manuscript received November 10, 2012; revised March 31, 2013; accepted June 17, 2013. The associate editor coordinating the review of this paper and approving it for publication was M. L. Merani.

A. Helmy and T. Le-Ngoc are with the Department of Electrical and Computer Engineering, McGill University, Montréal, QC, H3A 0E9, Canada (e-mail: amir.helmy@mail.mcgill.ca; tho-le.ngoc@mcgill.ca).

L. Musavian is with the School of Computing and Communications, InfoLab21, Lancaster University, Lancaster, LA1 4WA, United Kingdom (e-mail: l.musavian@lancaster.ac.uk).

This work was supported in part by the Natural Sciences and Engineering Research Council of Canada (NSERC). This paper was presented in part at the IEEE International Conference on Communications, Budapest, Hungary, 2013.

Digital Object Identifier 10.1109/TWC.2013.080113.120767

channels. In [8], energy-efficient link adaptation is addressed for frequency-selective fading channels, where iterative algorithms were developed to obtain the optimal solution. Energy-efficient link adaptation is also studied in [9] for a delay-unconstrained transmission on a frequency-selective parallel channel with sum rate-dependent circuit power, whereby a concave-convex fractional programming approach is used to solve the corresponding optimization problem.

By employing the EC formulation rather than the Shannon capacity, the rate-energy tradeoff of flat-fading channels under delay-outage probability constraints has been analyzed in [12], [13]. The considered models assume that the system operates under queuing constraints in the form of limitations on buffer violation probabilities. Specifically, [12] determines the minimum bit energy required to satisfy a certain delay constraint where the analysis has only been carried out in the low-power and wideband regimes. On the other hand, the studies in [12] and [13] did not develop a power allocation for optimizing the EE, nor did they consider the circuit power in their corresponding power models. An energy-efficient power allocation for delay-limited systems over flat-fading channels is proposed in [14] when taking into account the effect of the circuit power consumption on the maximum achievable EE.

In this paper, we develop an optimal energy-efficient power allocation strategy for a point-to-point multicarrier link over a frequency-selective fading channel under a target delay-outage probability constraint. First, by integrating the concept of EC with EE, the power adaptation policy aims at maximizing the system QoS-driven EE, defined by the ratio of the EC to the total expenditure power in units of b/J/Hz. The total power dissipation model includes a constant circuit power and a transmission power scaled by the power amplifier efficiency. Since independent subcarrier optimization does not provide an optimum EC maximization [3], it also cannot yield an optimal EE strategy. Therefore, a joint optimization over both frequency and time is formulated. To solve the underlying optimization problem using fractional programming, we start by proving that the objective function is a quasi-concave function of the transmit power allocations, and, as such, any stationary point is a global maximum. Next, we break down the problem into two main steps. In the first step, we find the average sum power needed to maximize the QoS-driven EE without any transmit power constraint. Then, in the second step, a power constraint is introduced and the transmit power is distributed optimally according to the constraint and the average sum power determined in the first step. The mathematical analysis provides insight into how the subcarrier powers should be chosen to optimize the QoS-driven EE. Specifically, the optimal subcarrier power allocation is determined as a function of the subchannel power gains, as well as the delay-QoS requirement. The derived scheme indicates that when the delay requirement becomes more stringent, the instantaneous transmission power converges accordingly from traditional water-filling to the channel inversion with fixed rate transmission. Furthermore, the trade-off between SE and EE in delay-limited multicarrier systems is analyzed by comparing the performances of the corresponding optimum power schemes. Using numerical analysis, we finally study the impact of the delay requirement, circuit power, transmit

power constraint, and frequency selectivity on the rate-energy tradeoff.

The rest of this paper is organized as follows. In Section II, we describe a generic multicarrier wireless system model, along with its underlying assumptions and parameters, where the framework for delay-QoS provisioning is highlighted. Then, in Section III, we first formulate the energy-efficient optimization problem under both independent and joint subcarrier allocations, wherein a jointly optimal power allocation policy is derived to maximize the QoS-driven EE of the multicarrier system without any power constraint. Next, we consider the scenario where the average sum power is limited and accordingly determine the power allocation that maximizes the system QoS-driven EE with sum power constraint. Finally, simulation results and conclusions are presented in Section IV.

II. SYSTEM MODEL

A. Multicarrier Transmission Model

We consider a point-to-point link over a wireless frequency-selective fading channel with a total bandwidth of B . Due to frequency selectivity, a multicarrier system is employed wherein N multiple subcarriers, each with a bandwidth of B/N , are used for transmission from the transmitter to the receiver. The general block diagram of the system model is illustrated in Fig. 1(a). In this model, the upper-layer data traffic enters a FIFO buffer at a constant arrival rate. The discrete-time channel input-output relation during the i^{th} multicarrier symbol is given by

$$y_n[i] = h_n[i]x_n[i] + n_n[i], \quad (1)$$

where $y_n[i]$, $x_n[i]$, $h_n[i]$ and $n_n[i]$ are the channel output, channel input, fading channel response and complex noise at the n^{th} subcarrier, respectively. The system is assumed to have ideal Nyquist transmission symbol rate with $T_s = \frac{N}{B}$ being the multicarrier symbol period. The choice of N depends on how frequency-selective is the fading channel such that each subcarrier undergoes independent frequency-flat fading.

The channel is considered to experience block fading where the channel gains of the N subcarriers are invariant during each fading-block, but change independently from one block to other. The length of each fading-block, denoted by T_f , is assumed to be an integer multiple of T_s . Denote the n^{th} subchannel power gain at block-index t by $\{\gamma_n[t] = |h_n[t]|^2, n \in \mathcal{N}_0\}$, where $\mathcal{N}_0 = \{1, 2, \dots, N\}$ represents the set of all potential subcarriers. The joint probability density function (pdf) of the subchannel power gains $\gamma[t] = [\gamma_1[t] \ \gamma_2[t] \ \dots \ \gamma_N[t]]$ is then given by $\rho(\gamma)$. Each subcarrier is also assumed to experience independent identically distributed (i.i.d.) additive white Gaussian noise with power spectral density $\frac{\eta_0}{2}$.

We further assume that the transmitter has perfect knowledge of the instantaneous CSI fed back from the receiver without delay. Based on a given QoS constraint, represented by the QoS exponent θ (to be detailed in the following subsections II-B and II-C), and the instantaneous subchannel power gains $\gamma[t]$, adaptive modulation and coding (AMC) is first applied at the transmitter side to enhance the system performance, followed by a subcarrier power allocation policy

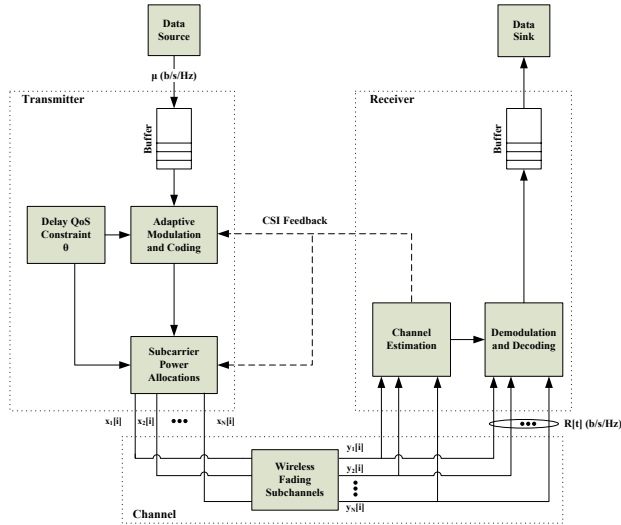


Fig. 1(a): Multicarrier System Model.

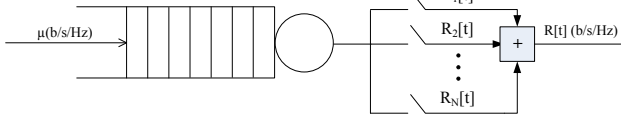


Fig. 1(b): Queueing System Model.

Fig. 1: Multicarrier System.

$\{P_n(\theta, \gamma[t]), \forall n \in \mathcal{N}_0\}$. Although the power allocation is based on an interval duration of T_f , it is important to note that the transmitter buffer operates at the multicarrier symbol transmission rate of $\frac{1}{T_s}$ as shown in (1). At the receiver, the subchannel power gains are perfectly estimated and the received symbols are then demodulated and decoded accordingly. During the t^{th} fading-block, the instantaneous received signal-to-noise ratio at the n^{th} subcarrier can be expressed as

$$\text{SNR}_n[t] = P_n(\theta, \gamma[t]) \cdot \frac{\gamma_n[t]}{P_L \eta_0 \left(\frac{B}{N}\right)}, \quad \forall n \in \mathcal{N}_0, \quad (2)$$

where $\frac{B}{N}$ is the subcarrier bandwidth and P_L is the distance-based path loss power. Assuming AMC can achieve Shannon capacity, the total instantaneous service rate of the multicarrier system at the t^{th} fading-block is

$$R[t] = \frac{1}{N} \sum_{n=1}^N \log_2 \left(1 + \frac{P_n(\theta, \gamma[t]) \gamma_n[t]}{P_L \eta_0 \left(\frac{B}{N}\right)} \right), \quad (\text{b/s/Hz}). \quad (3)$$

B. Effective Capacity

To analyze the buffer overflow probability, and indirectly the delay-outage probability, we apply the link-layer EC notion introduced in [2], where a wireless link is characterized by the QoS exponent θ of the connection, and the probability of nonempty buffer. The EC function specifies the maximum constant arrival rate that the system can support to maintain a target delay requirement indicated by θ . The queue model of our multicarrier system is depicted in Fig. 1(b). The source data rate is fixed to a constant μ (b/s/Hz), whereas the stationary and ergodic service process $R[t]$ is variable.

Given that the Gärtner-Ellis Theorem assumptions in [1] are satisfied, the EC function of the underlying multicarrier system with i.i.d. subchannels can be expressed as

$$E_c(\theta) = -\frac{1}{\theta T_f B} \ln \left(\mathbb{E} \left[e^{-\theta B T_f R[t]} \right] \right), \quad (\text{b/s/Hz}), \quad (4)$$

where the EC is normalized to the fading-block length T_f and system bandwidth B . Substituting the expression of $R[t]$ from (3) into (4), the resulting EC is obtained as

$$E_c(\theta, \mathbf{P}(\theta, \gamma)) = -\frac{1}{\alpha} \log_2 \left(\mathbb{E}_\gamma \left[\prod_{n=1}^N \left(1 + \frac{P_n(\theta, \gamma) \gamma_n}{P_L \eta_0 \left(\frac{B}{N}\right)} \right)^{-\frac{\alpha}{N}} \right] \right), \quad (\text{b/s/Hz}), \quad (5)$$

where $\mathbf{P}(\theta, \gamma) = [P_1(\theta, \gamma) \ P_2(\theta, \gamma) \ \dots \ P_N(\theta, \gamma)]$ denotes a $N \times 1$ vector of subcarrier power allocations, $\alpha \equiv \frac{\theta T_f B}{\ln(2)}$, $\mathbb{E}_\gamma[\cdot]$ indicates the expectation over the pdf of γ and the time index t is omitted for notational simplicity without causing ambiguity.

C. Delay-outage Probability

Based on the large-deviation principle theorem and assuming that the steady-state queue length exists, the probability that the queue length $Q(t)$ exceeds a certain threshold x decays exponentially fast as the threshold x increases [1], as such

$$-\lim_{x \rightarrow \infty} \frac{\ln(\Pr\{Q(\infty) \geq x\})}{x} = \theta. \quad (6)$$

Large and small values of θ correspond to fast and slow decaying rates indicating stringent and loose QoS requirements, respectively. For example, when $\theta \rightarrow 0$, the system can tolerate an arbitrarily long delay, whereas the system cannot tolerate any delay when $\theta \rightarrow \infty$. The delay-outage probability, defined as the probability that the delay exceeds a maximum delay-bound D_{\max} , can be estimated as [2]

$$\Pr\{\text{Delay} \geq D_{\max}\} \simeq \gamma^{(c)}(\mu) e^{-\mu \theta(\mu) D_{\max}}, \quad (7)$$

where D_{\max} is expressed in units of $1/B$. For a given μ , $\gamma^{(c)}(\mu) \equiv \Pr\{Q(t) \geq 0\}$ is the probability that the buffer is nonempty at a time t and can be approximated as the ratio of the constant arrival rate to the average service rate [1], i.e., $\gamma^{(c)}(\mu) \simeq \frac{\mu}{\mathbb{E}[R[t]]}$, while $\theta(\mu)$ is simply the QoS exponent θ determined by the inverse function of the EC, $E_c^{-1}(\mu)$. Hence, to meet a target delay-probability limit P_{out} , i.e., $\Pr\{\text{Delay} \geq D_{\max}\} \leq P_{\text{out}}$, a source needs to limit its data rate to a maximum of μ , where μ is the solution to (7).

III. QOS-DRIVEN ENERGY-EFFICIENT POWER ALLOCATION

Assuming perfect CSI at the transmitter, an opportunistic power adaptation scheme can be developed to minimize the energy consumption per bit, or equivalently, maximize the transmitted data per unit energy, while satisfying a target delay-outage probability limit. The metric of interest in this case is the QoS-driven EE for delay-limited systems defined as the ratio of the EC to the total expenditure power. The total

power dissipation model includes a constant circuit power P_C and a transmission power scaled by the power amplifier efficiency ε . The rate-independent circuit power P_C corresponds to the power dissipated in device electronics. Accordingly, the QoS-driven EE is mathematically represented as

$$\text{EE}(\theta) = \frac{-\frac{1}{\alpha} \log_2 \left(\mathbb{E}_\gamma \left[\prod_{n=1}^N \left(1 + \frac{N P_n(\theta, \gamma) \gamma_n}{K_L} \right)^{-\frac{\alpha}{N}} \right] \right)}{P_C + \varepsilon \cdot \mathbb{E}_\gamma \left[\sum_{n=1}^N P_n(\theta, \gamma) \right]}, \quad (8)$$

where $K_L \equiv P_L N_0 B$ is a loss factor denoting the product of path loss and noise power. In order to normalize the system performance with respect to K_L , we define $P_n^R(\theta, \gamma) \equiv \frac{P_n(\theta, \gamma)}{K_L}$ as the ratio of the transmit power at the n^{th} subcarrier to the path loss and noise power. Thus, the EC formula can be expressed as

$$\begin{aligned} E_c(\theta, \mathbf{P}^R(\theta, \gamma)) \\ = -\frac{1}{\alpha} \log_2 \left(\mathbb{E}_\gamma \left[\prod_{n=1}^N \left(1 + N \cdot P_n^R(\theta, \gamma) \gamma_n \right)^{-\frac{\alpha}{N}} \right] \right), \end{aligned} \quad (9)$$

where $\mathbf{P}^R(\theta, \gamma) = [P_1^R(\theta, \gamma) \quad P_2^R(\theta, \gamma) \quad \dots \quad P_N^R(\theta, \gamma)]$.

A. Independent Subcarrier Optimization

As a reference, we first consider a simple EE power allocation scheme whereby the power is equally divided over the N subchannels such that the power allocation in each subcarrier P_n^R can be independently performed and, thus, it only depends on its corresponding channel power gain γ_n . For i.i.d. fading over the subcarriers, this is equivalent to maximizing the total EE of the multicarrier system using the optimal power adaptation policy for the single carrier flat-fading transmission proposed in [14]. In this case, the EC of N independently optimized i.i.d. subchannels is given by $E_c^{(N)}(\theta) = E_c^{(1)}\left(\frac{\theta}{N}\right)$ [3], where $E_c^{(1)}(\theta)$ is the normalized EC of a flat-fading channel with bandwidth B . Hence, the EE maximization can be expressed as

$$\max_{P^R \geq 0} \frac{1}{\varepsilon K_L} \cdot \frac{E_c^{(1)}\left(\frac{\theta}{N}\right)}{P_{C_r} + \mathbb{E}_\gamma [P^R(\theta, \gamma)]}, \quad (10)$$

where $P^R(\theta, \gamma)$ is the total power spend over a bandwidth B , γ is the channel power gain of a single carrier flat-fading and $P_{C_r} = \frac{P_C}{\varepsilon K_L}$ is the normalized circuit power. The corresponding subcarrier power allocations can be obtained using [4], [14] as

$$P_n^R(\theta, \gamma_n) = \frac{1}{N} \left[\frac{1}{\delta^{\frac{N}{\alpha+N}} \gamma_n^{\frac{\alpha}{\alpha+N}}} - \frac{1}{\gamma_n} \right]^+, \quad n \in \mathcal{N}_0, \quad (11)$$

where $[x]^+ = \max(0, x)$ and δ is a cutoff threshold that can be found numerically to maximize (10).

It was shown in [3] that maximizing the EC at each subchannel independently, using the optimal power adaptation policy for the single channel transmission, does not yield a SE-optimal power scheme. In fact, by using the independent allocation over N i.i.d. subchannels, the resulting EC, $E_c^{(N)}(\theta)$, converges to zero as $\theta \rightarrow \infty$ for any finite N . In turn, by applying the independent EE optimization approach in (11)

to our underlying multicarrier system, the achievable EE at very stringent θ is expected to converge to zero for any finite power. Hence, independently optimizing the power allocated to the subcarriers can not yield an EE-optimal power scheme. In the following sections, we propose an optimal EE power allocation policy where the power is jointly distributed over both frequency and time.

B. Jointly Optimal Energy-Efficient Power Allocation Policy without Transmit Power Constraint

First, the unconstrained optimization problem is tackled without considering any input transmit power constraint, serving as a milestone towards finding an EE-optimal power allocation subject to an average sum power constraint. To maximize the QoS-driven EE, the optimization problem can now be formulated as follows

$$\text{EE}^{\text{opt}}(\theta) = \max_{P_n^R \geq 0, n \in \mathcal{N}_0} \frac{1}{\varepsilon K_L} \cdot \frac{E_c(\theta, \mathbf{P}^R(\theta, \gamma))}{P_{C_r} + \mathbb{E}_\gamma \left[\sum_{n=1}^N P_n^R(\theta, \gamma) \right]}. \quad (12)$$

In [15], a mathematical framework called fractional programming is provided to solve optimization problems where the objective function is a ratio of two real-valued functions. Specifically, the authors showed that a broad class of EE maximization problems can be solved efficiently provided the rate is a concave function of the transmit power. To use this solution methodology to solve our optimization problem in (12), we prove that the EC, $E_c(\theta, \mathbf{P}^R(\theta, \gamma))$, is concave on the domain where \mathbf{P}^R is defined by verifying the convexity of $f(\mathbf{P}^R) = \ln \left(\mathbb{E}_\gamma \left[\prod_{n=1}^N \left(1 + N \cdot P_n^R(\theta, \gamma) \gamma_n \right)^{-\frac{\alpha}{N}} \right] \right)$. For a multi-variable function to be convex, we need to show that the Hessian of $f(\mathbf{P}^R)$ is positive semi-definite (PSD). We start by introducing the following theorem.

Theorem 1: The Hessian of the function $f(\mathbf{P}^R)$, denoted by $\nabla^2 f(\mathbf{P}^R)$, is an $N \times N$ real symmetric matrix whose eigenvalues are $b - a$ and $b + (N - 1)a$ with $a \equiv \frac{\partial^2 f(\mathbf{P}^R)}{\partial P_i^R \partial P_j^R}$ and $b \equiv \frac{\partial^2 f(\mathbf{P}^R)}{\partial P_i^R^2}, \forall i, j = 1, 2, \dots, N, i \neq j$.

Proof: The proof is provided in Appendix A. ■

Using the fact that a symmetric matrix is PSD if and only if all its eigenvalues are positive, we therefore proceed with the following theorem to show that both eigenvalues are indeed positive.

Theorem 2: All the eigenvalues of $\nabla^2 f(\mathbf{P}^R)$, namely $b - a$ and $b + (N - 1)a$, are positive, and in turn $\nabla^2 f(\mathbf{P}^R)$ is PSD.

Proof: The proof is provided in Appendix B. ■

Accordingly, the objective function in (12) is a ratio of a concave to an affine function in $\mathbf{P}^R(\theta, \gamma)$, and hence a global maximum can be obtained by fractional programming. Specifically, by using the variable transformation $t = \left(P_{C_r} + \mathbb{E}_\gamma \left[\sum_{n=1}^N P_n^R(\theta, \gamma) \right] \right)^{-1}$, we get an equivalent concave optimization problem

$$\max_{P_n^R \geq 0, n \in \mathcal{N}_0} t \cdot E_c(\theta, \mathbf{P}^R(\theta, \gamma)) \quad (13a)$$

$$\text{subject to } t \left(P_{C_r} + \mathbb{E}_\gamma \left[\sum_{n=1}^N P_n^R(\theta, \gamma) \right] \right) = 1. \quad (13b)$$

Since (13a) is a concave function and the equality constraint in (13b) is an affine function, the Karush-Kuhn-Tucker (KKT) conditions are both necessary and sufficient for optimality. Introducing a Lagrangian multiplier $\lambda \geq 0$ for that equality constraint and $\{v_n \geq 0, n = 1, 2, \dots, N\}$ for the N inequality constraints $\{P_n^R \geq 0, n \in \mathcal{N}_0\}$, the Lagrangian is

$$\mathcal{L}(P_n^R, t, \lambda, v_n) = -t \cdot E_c(\theta, \mathbf{P}^R(\theta, \gamma)) + \lambda \left[t \left(P_{C_R} + \mathbb{E}_\gamma \left[\sum_{n=1}^N P_n^R \right] \right) - 1 \right] - \sum_{n=1}^N v_n P_n^R,$$

where, hereafter, $P_n^R(\theta, \gamma)$ is denoted as P_n^R for notational simplicity. Also, the underlying KKT conditions are

$$(P_n^R)^* \geq 0, \quad \forall n \in \mathcal{N}_0 \quad (14a)$$

$$t \left(P_{C_R} + \mathbb{E}_\gamma \left[\sum_{n=1}^N (P_n^R)^* \right] \right) - 1 = 0 \quad (14b)$$

$$-t \frac{dE_c(\theta, \mathbf{P}^R)}{d(P_n^R)^*} + \lambda t \int_0^\infty \dots \int_0^\infty \rho(\gamma) d\gamma_1 \dots d\gamma_N = v_n. \quad (14c)$$

Based on the concept of complementary slackness, if the strict inequality $P_n^R > 0$ holds for any $n = 1, 2, \dots, N$, then we have $v_n = 0$. Thus, the following two cases need to be considered to find the optimal power allocations $(P_n^R)^*$.

1) *Case 1:* $P_n^R > 0, \forall n = 1, 2, \dots, N$: As such, all subcarriers are allocated non-zero power for transmission. Hence, based on the complementary slackness condition, all Lagrangian multipliers $\{v_n\}_{n=1}^N$ must be equal to zero. Then, the third condition of (14c) can be simplified as

$$(1 + N \cdot P_n^R \gamma_n)^{-\frac{\alpha}{\alpha+1}} \prod_{i \neq n} (1 + N \cdot P_i^R \gamma_i)^{-\frac{\alpha}{\alpha+1}} = \frac{\lambda \kappa \ln(2)}{\gamma_n}, \quad \forall n \in \mathcal{N}_0, \quad (15)$$

with $\kappa = \mathbb{E}_\gamma \left[\prod_{n=1}^N (1 + N P_n^R \gamma_n)^{-\frac{\alpha}{\alpha+1}} \right]$. Note that the power allocation of the n^{th} subcarrier P_n^R depends on all the subchannel power gains γ , rather than just the n^{th} subchannel γ_n . The resulting expression can be solved by multiplying the right- and left-hand sides of the N equations in (15) together. In turn, the optimal power allocations can be obtained as

$$P_n^R = \frac{1}{N} \left[\frac{1}{\delta^{\frac{1}{\alpha+1}} \prod_{i \in \mathcal{N}_0} \gamma_i^{\frac{\alpha}{(\alpha+1)N}}} - \frac{1}{\gamma_n} \right], \quad n \in \mathcal{N}_0, \quad (16)$$

where $\delta \equiv \lambda \kappa \ln(2)$ is a cut-off threshold below which no power is allocated for transmission. The above power allocations are optimal if and only if each subcarrier is assigned a power allocation that is strictly positive, i.e., $P_n^R > 0 \forall n = 1, 2, \dots, N$. In other words, the solution is optimal only if $\mathcal{N}_1 = \mathcal{N}_0 = \{1, 2, \dots, N\}$, where \mathcal{N}_1 is defined as

$$\mathcal{N}_1 = \left\{ n \in \mathcal{N}_0 \left| \frac{1}{N} \left[\frac{1}{\delta^{\frac{1}{\alpha+1}} \prod_{i \in \mathcal{N}_0} \gamma_i^{\frac{\alpha}{(\alpha+1)N}}} - \frac{1}{\gamma_n} \right] \geq 0 \right. \right\}. \quad (17)$$

On the other hand, if one or more subcarriers are assigned non-positive power allocations such that $\mathcal{N}_1 \subset \mathcal{N}_0$, then we need to account for a different case as outlined below.

2) *Case 2:* $P_m^R = 0$ for some $m \in 1, 2, \dots, N$ such that $\mathcal{N}_1 \subset \mathcal{N}_0$: If there exists some $P_m^R \leq 0$, then we have to find the set of subcarriers to which zero power should be assigned. Since the structure of the power allocation in (16) is similar to the one derived in [3], Lemma 1 of [3] is applicable to our optimization problem. This lemma states that all the power must be assigned to the subchannels that belong to \mathcal{N}_1 . Therefore, using Lemma 1, if $m \notin \mathcal{N}_1$, then P_m^R must be zero. In fact, this indicates that the proposed allocation algorithm that excludes subcarrier m whose $P_m^R \leq 0$ is indeed optimal. Thus, all the power must be allocated to the subcarriers that belong to \mathcal{N}_1 wherein the values of P_n^R must be reproduced for any subcarrier $n \in \mathcal{N}_1$, while setting $P_m^R = 0$ if $m \notin \mathcal{N}_1$. Consequently, this yields an optimization problem that has a similar structure to the original maximization, but the optimization space reduces from \mathcal{N}_0 to \mathcal{N}_1 as such

$$\max_{P_n^R \geq 0, n \in \mathcal{N}_1} \frac{-\frac{1}{\alpha} \log_2 \left(\mathbb{E}_\gamma \left[\prod_{n \in \mathcal{N}_1} (1 + N \cdot P_n^R \gamma_n)^{-\frac{\alpha}{\alpha+1}} \right] \right)}{P_{C_R} + \mathbb{E}_\gamma \left[\sum_{n \in \mathcal{N}_1} P_n^R \right]}. \quad (18)$$

Hence, if the strict inequality $P_n^R > 0$ holds for all $n \in \mathcal{N}_1$, then, the resulting optimization can be solved exactly like before. Otherwise, if not all the subcarriers $n \in \mathcal{N}_1$ satisfy $P_n^R > 0$, then \mathcal{N}_1 must be further partitioned by repeating the above process recursively until a set \mathcal{N}^* can be identified in which all subcarriers are allocated positive powers (i.e., if $\mathcal{N}_k = \mathcal{N}_{k-1} = \{n \in \mathcal{N}_k | P_n^R > 0\}$, then $\mathcal{N}^* = \mathcal{N}_k$). After obtaining \mathcal{N}^* , the optimal power allocations are computed as

$$P_n^R = \begin{cases} \frac{1}{N} \left[\frac{1}{\delta^{\frac{1}{N+\alpha N^*}} \prod_{i \in \mathcal{N}^*} \gamma_i^{\frac{\alpha}{N+\alpha N^*}}} - \frac{1}{\gamma_n} \right], & n \in \mathcal{N}^* \\ 0, & \text{otherwise,} \end{cases} \quad (19)$$

where $N^* = |\mathcal{N}^*|$ represents the cardinality of \mathcal{N}^* . Since all unknowns have been expressed as functions of λ , this reduces to finding the optimal $\lambda^* > 0$ from the condition

$$\nabla_t \mathcal{L} = -E_c(\theta, (\mathbf{P}^R)^*) + \lambda^* \left(P_{C_R} + \mathbb{E}_\gamma \left[\sum_{n=1}^N (P_n^R)^* \right] \right) = 0. \quad (20)$$

λ^* can be determined numerically using a bisection root-finding search algorithm, and in turn, the cut-off threshold δ^* is obtained. Now, the maximum achievable optimal QoS-driven EE in b/J/Hz can then be calculated as

$$EE^{\text{opt}}(\theta) = \frac{\lambda^*}{\varepsilon K_L}. \quad (21)$$

Whereas the complexity of the independent subcarrier optimization of Section III-A grows linearly with the number of subcarriers N , i.e., of $O(N)$, the complexity of the jointly optimal power allocation is of $O(\sum_{k=0}^K |\mathcal{N}_k|) = O(dN)$ where $K+1 \leq N$ is the required number of recursions to obtain \mathcal{N}^* and $1 \leq d \leq (N+1)/2$. In other words, in the worst-case scenario where \mathcal{N}_k always has one less element than \mathcal{N}_{k-1} (i.e., $|\mathcal{N}_k| = |\mathcal{N}_{k-1}| - 1, \forall k = 1, \dots, N-1$), N recursions are required and hence, the worst-case complexity is of $O(1 + 2 + \dots + N) = O\left(\frac{N(N+1)}{2}\right) \approx O(N^2)$.

The analytical results show that the derived energy-efficient power allocation in (19) has a structure that is identical to the QoS-driven spectral-efficient power adaptation of [3], but with a different cut-off threshold. In fact, given a power allocation strategy that maximizes the QoS-driven EE without transmit power constraint, one can show that this allocation is essentially the same as the power allocation for maximizing the EC with a sum power constraint $\overline{P}_{\text{un}}^* = \mathbb{E}_{\gamma} \left[\sum_{n=1}^N (P_n^{\text{R}})^* \right]$. In other words, our EE maximization problem can be solved in two steps. In the first step, we compute the optimal δ^* by solving (20). Next, we can determine the corresponding average sum power $\overline{P}_{\text{un}}^*$ at which the maximum EE will be achieved by inserting δ^* into

$$\overline{P}_{\text{un}}^* = \mathbb{E}_{\gamma} \left[\sum_{n=1}^N (P_n^{\text{R}}) \right] \Big|_{\delta=\delta^*}. \quad (22)$$

Hence, the optimum value for the denominator of the EE objective function in (12) is now fixed to $P_{\text{C}} + \overline{P}_{\text{un}}^*$. Accordingly, the EE maximization reduces to maximizing the EC with an average input power limit set to $\overline{P}_{\text{un}}^*$. As such, in the second step, the transmit power is optimally distributed over frequency and time according to $\overline{P}_{\text{un}}^*$ found earlier in the first step.

Since the underlying setup is a multicarrier system, this power strategy can be essentially viewed as a subcarrier selection scheme where a subset of the subcarriers is selected for transmission while excluding those unwanted subcarriers based on the channel statistics and delay requirement. As we will see later in Section IV, when the QoS exponent θ increases from zero to infinity, the instantaneous transmission power is shown to converge accordingly from traditional water-filling to channel inversion with fixed rate transmission.

C. Energy-Efficient Power Allocation Policy with Average Sum Power Constraint

After solving the power-unconstrained problem in the previous section, we will now turn to the scenario where the average sum transmit power is limited by \overline{P} . Consequently, the optimization problem can now be formulated as follows:

$$\begin{aligned} \max_{P_n^{\text{R}} \geq 0, n \in \mathcal{N}_0} & \frac{1}{\varepsilon K_{\text{L}}} \cdot \frac{E_{\text{c}}(\theta, \mathbf{P}^{\text{R}}(\theta, \gamma))}{P_{\text{C}_{\text{R}}} + \varepsilon \cdot \mathbb{E}_{\gamma} \left[\sum_{n=1}^N P_n^{\text{R}} \right]} \\ \text{subject to} & \mathbb{E}_{\gamma} \left[\sum_{n=1}^N P_n^{\text{R}} \right] \leq \overline{P}, \end{aligned} \quad (23)$$

with $\overline{P} = \frac{\overline{P}}{K_{\text{L}}}$ being the average sum transmit power constraint scaled by the loss factor K_{L} . Generally speaking, the EE maximization problem is different from the SE maximization problem in the sense that the transmit power constraint is not necessarily satisfied with equality in EE-optimal systems as opposed to the SE-optimal case.

First, we consider the scenario where $\overline{P}_{\text{un}}^* \leq \overline{P}$ such that the transmit power limit is actually higher than the required power for maximizing the unconstrained QoS-driven EE. Consequently, the power allocation for maximizing the unconstrained QoS-driven EE does indeed satisfy the average sum power constraint, and thus, the maximum QoS-driven EE

for the power-constrained problem is achieved using the same optimal solution as the unconstrained problem (i.e., $\overline{P}_{\text{un}}^*$).

Second, the scenario where $\overline{P}_{\text{un}}^* > \overline{P}$ is studied such that the solution obtained for the unconstrained problem is no longer valid. Hence, in this case, we have the following theorem to formally characterize this problem.

Theorem 3: The constrained QoS-driven EE optimization problem with a maximum power limit $\overline{P}^{\text{R}} < \overline{P}_{\text{un}}^*$ is equivalent to an EC maximization with sum power constraint \overline{P}^{R} .

Proof: The proof is provided in Appendix C. ■

Therefore, the optimal EE in this scenario is achieved by consuming all of the available power \overline{P}^{R} . In other words, the power allocation that maximizes the constrained QoS-driven EE turns out to be the same as the power adaptation policy proposed in [3] to maximize the EC with an average power constraint, as given below:

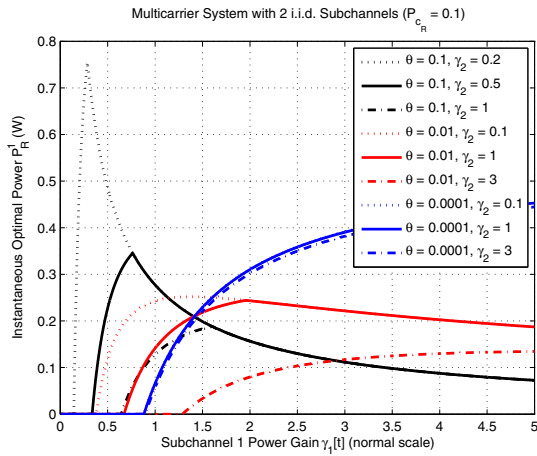
$$\begin{aligned} \max_{P_n^{\text{R}} \geq 0, n \in \mathcal{N}_0} & E_{\text{c}}(\theta, \mathbf{P}^{\text{R}}(\theta, \gamma)) \\ \text{subject to} & \mathbb{E}_{\gamma} \left[\sum_{n=1}^N P_n^{\text{R}}(\theta, \gamma) \right] \leq \overline{P}^{\text{R}} \end{aligned} \quad (24)$$

IV. ILLUSTRATIVE RESULTS

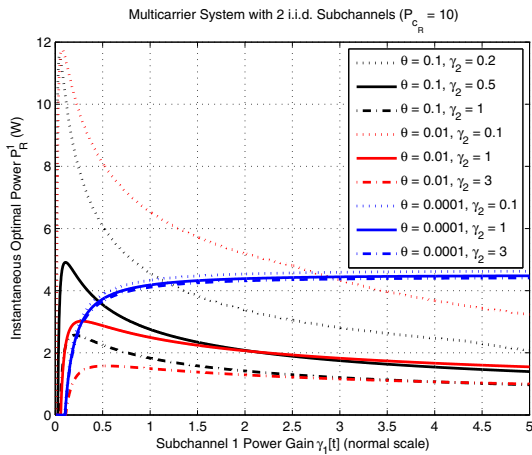
In this section, we simulate a delay-constrained multicarrier system to evaluate the performance of the proposed jointly EE-optimal power allocation and investigate the impact of the circuit power, frequency selectivity, and transmit power constraint on the achievable EE. In addition, the proposed scheme is compared with both the independent subcarrier EE-based optimization approach and the SE-based power adaptation of [3] in terms of EE as well as EC, whereby the rate-energy tradeoff is illustrated. We consider a Rayleigh fading channel such that the subcarrier power gains $\gamma_1, \gamma_2, \dots, \gamma_n$ are exponentially distributed with unit mean. In the following results, unless otherwise specified, the scaled circuit power $P_{\text{C}_{\text{R}}}$ is considered to be 0.1, the average sum power constraint is assumed to be $\overline{P}^{\text{R}} = 1\text{W}$, and $BT_{\text{f}} = 200$.

We start by examining the characteristics of the jointly optimal power adaptation policy in (19) by plotting the subcarrier power allocation P_1^{R} as a function of the channel power gains γ and the QoS exponent θ . Fig. 2a indicates that when θ increases, the instantaneous transmission power converges accordingly from traditional water-filling to channel inversion with fixed rate transmission. For instance, in systems with tight delay requirements, e.g., $\theta = 0.1$, the power increases to some certain threshold and then it starts to decrease with the channel power gain. Next, we investigate the impact of the circuit power $P_{\text{C}_{\text{R}}}$ on the optimal instantaneous power. We conclude from Fig. 2b that as the circuit power increases from $P_{\text{C}_{\text{R}}} = 0.1$ to $P_{\text{C}_{\text{R}}} = 10$, the instantaneous power curves become more steep and the cutoff thresholds decrease correspondingly. Therefore, in contrary to delay-unconstrained system, the structure of the QoS-driven EE-optimal power allocation is not a standard water-filling approach, but rather depends on both the circuit power and the delay requirement.

Fig. 3a shows the maximum achievable QoS-driven EE in b/J/Hz, averaged over 10^6 channel realizations, versus the QoS exponent θ for two jointly-optimal power allocation strategies, namely SE-based and EE-based schemes. To study



(a) $P_{C_R} = 0.1$.

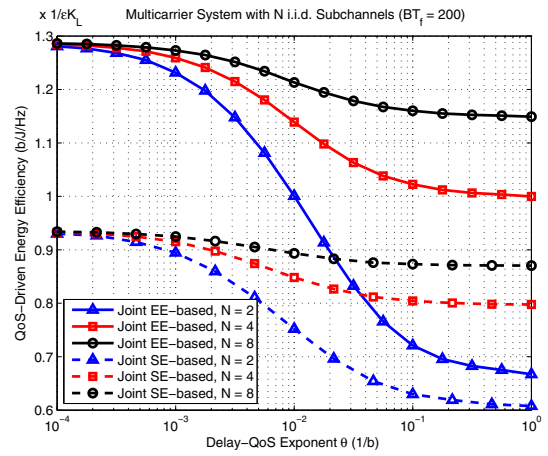


(b) $P_{C_R} = 10$.

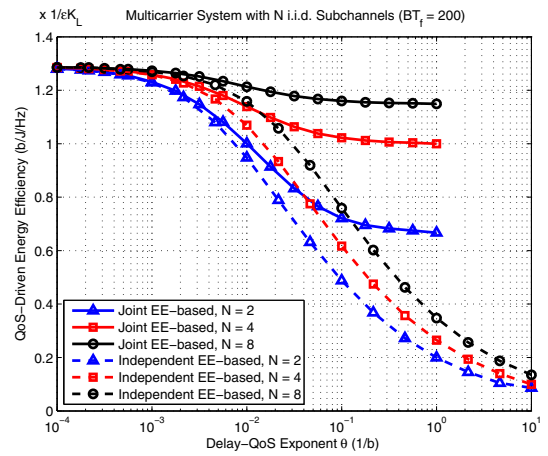
Fig. 2: Instantaneous optimal power P_1^R versus channel power gain $\gamma_1[t]$ for various $\gamma_2[t]$ and θ in Rayleigh fading channels.

the effect of the frequency selectivity on EE, the curves are plotted for various number of subcarriers N . For a given channel bandwidth B , larger N indicates that the channel is more frequency-selective, and hence, narrower subcarriers are required to maintain frequency-flat fading subcarriers. The achievable EE is shown to decrease as the delay requirement becomes more stringent. The results show that the joint EE-based scheme provides significant EE gains over the SE-based system. In particular, for loose delay regimes, the gain in EE is as much as 40%, whereas the relative gain gets smaller as θ becomes more stringent. Fig. 3a also demonstrates that the relative EE gains increase with the frequency-selectivity. In other words, our proposed EE-based allocation is more beneficial in fading channels with higher frequency selectivity.

We then compare the EE of our proposed jointly optimal allocation with that of the independent subcarrier optimization in (10). From Fig. 3b, the achievable EE of the independent approach is shown to converge to zero for all N as $\theta \rightarrow \infty$, and hence, this simple scheme has a substantial loss in EE relative to the optimal strategy particularly when the delay constraint is stringent. For a given θ , the performance difference between the two schemes becomes more pronounced as N increases



(a) Jointly optimal EE- and SE-based allocations.



(b) Independent and jointly optimal EE-based allocations.

Fig. 3: Maximum achievable QoS-Driven EE of multicarrier system with N i.i.d. subcarriers.

(i.e. higher frequency-selectivity). This can be explained by the fact that the proposed jointly optimal EE-based power allocation can exploit the subchannel diversity. Furthermore, with fixed N , the relative degradation θ in the achievable EE is more remarkable for higher θ (i.e., more stringent delay-outage constraint). For instance, at $\theta = 10$ and $N = 8$, the EE of the proposed jointly EE-optimal power allocation scheme is about 6 times that of the simple independent subcarrier optimization scheme.

To better highlight the impact of the frequency-selectivity on the maximum achievable EE of our proposed scheme, we plot in Fig. 4 the optimum EE versus N for various θ . As N increases, the optimum EE increases for any given delay exponent θ until it saturates for larger values of N , where systems with more stringent delay requirements benefit the most from the frequency-selectivity. At large values of N , which is more practical in real-world scenarios, our scheme manages to achieve a fixed optimal EE regardless of the stringency of the delay constraint.

Fig. 5 plots the normalized EC of the multicarrier system versus θ . The results illustrate a clear trade-off between SE and EE where the increasing EE does indeed come at the

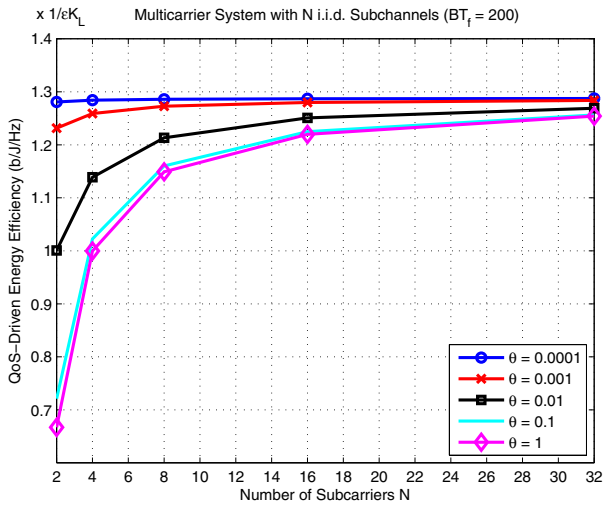
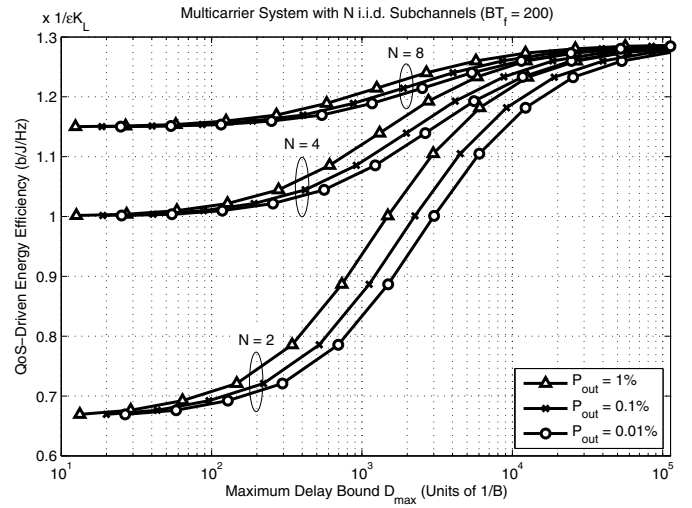


Fig. 4: Effect of N on maximum achievable EE for various θ .



(a) Proposed jointly optimal EE-based allocation.

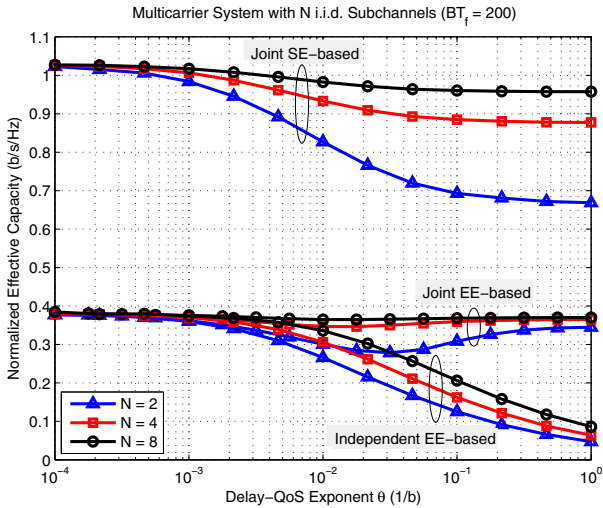
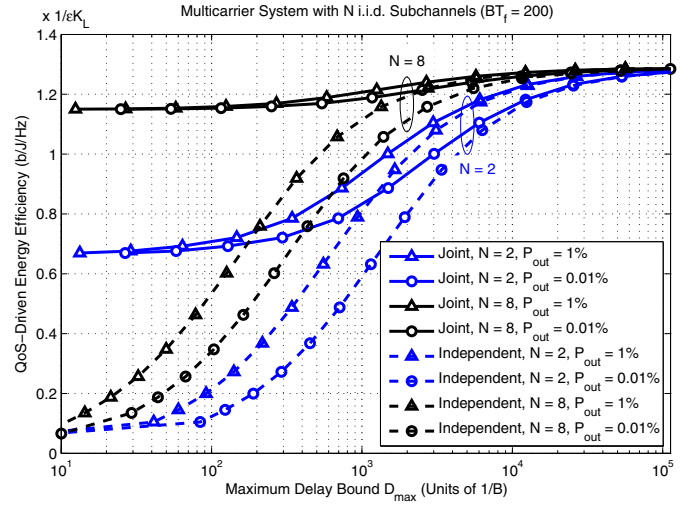


Fig. 5: Effective capacity of the Multicarrier System.



(b) Independent and jointly optimal EE-based allocations.

Fig. 6: Maximum achievable EE versus delay-bound for multicarrier system with N i.i.d. subcarriers.

cost of decreasing SE. In other words, we have to sacrifice some rate in order to maximize the EE of the multicarrier system. The amount of trade-off depends on θ and N , as well as on the scaled circuit power P_{C_R} . Specifically, the results show that there is more rate-energy tradeoff in fading channels with higher frequency selectivity. The achievable EC of the independent subcarrier EE-based optimization is similar to that of the jointly optimal allocation at low values of θ . However, unlike the joint strategy, the EC of the independent approach converges to zero for all N as $\theta \rightarrow \infty$.

Fig. 6a plots the maximum achievable QoS-driven EE of our proposed jointly optimal allocation versus the delay-bound D_{\max} for various target delay-outage probabilities P_{out} . The EE is shown to increase with increasing D_{\max} for any given P_{out} . In other words, as the delay violation limit is relaxed, our proposed scheme achieves better EE gains. In addition, for a particular N , the EE decreases gradually with diminishing outage probability, where, at low values of D_{\max} , all the curves converge to an EE level that increases with N . Fig. 6a also

indicates that the achievable EE becomes less sensitive to P_{out} as N increases. In Fig. 6b, we compare the maximum achievable EE of the independent and jointly optimal schemes as a function of D_{\max} for different P_{out} . In contrary to the jointly optimal scheme where the EE converges to a non-zero value as D_{\max} decreases, the EE of the independent subcarrier optimization scheme converges to zero for all N and P_{out} . In other words, for a given multicarrier system with a target delay-outage probability, the proposed jointly EE-optimal power allocation offers significant EE gains over the simple independent subcarrier optimization scheme.

Fig. 7 then shows the normalized EC against D_{\max} again for jointly-optimal EE-based power allocation with different outage probabilities. The behavior cannot be easily explained since different points employ different average powers. However, from these results, one can conclude that the required buffer size for a given source rate μ can be determined from the product of D_{\max} and μ . For example, for $N = 2$, with $\mu = 0.35$ b/s/Hz, the required buffer size to meet a delay-

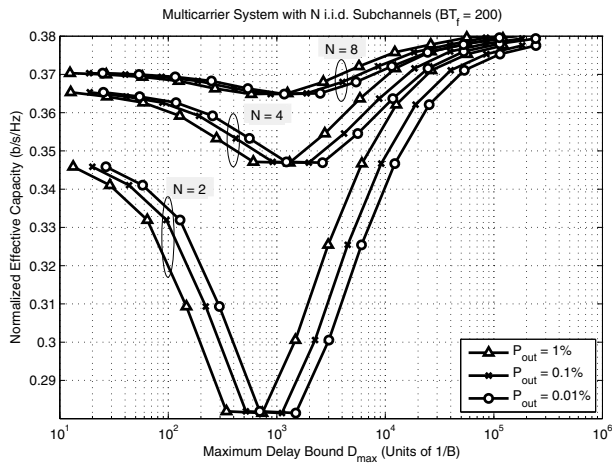


Fig. 7: Normalized effective capacity versus maximum delay bound for multicarrier system with N i.i.d. subcarriers using proposed jointly optimal EE-based allocation.

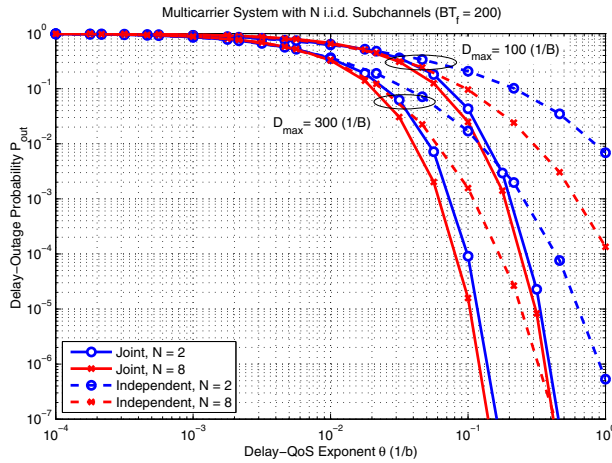


Fig. 8: Delay-outage probability versus QoS exponent for multicarrier system with N subcarriers.

outage P_{out} of 1% is about 2500 bits.

Next, Fig. 8 plots the delay-outage probability P_{out} versus θ for independent and jointly-optimal EE-based allocations with various D_{max} . For a given D_{max} , the delay-outage probability is shown to decrease with the QoS exponent, where the independent approach experiences lower decaying rates compared to the joint allocation particularly at high values of θ . Also, the outage probability of both power allocations diminishes with increasing D_{max} . Furthermore, for a given D_{max} , P_{out} decreases as N increases where the reduction in the delay-outage probability is more pronounced in the independent optimization approach, as opposed to the joint scheme which is less sensitive to N .

In Fig. 9, we plot the EC against the scaled sum power constraint $\overline{P^R}$ for $N = 2$ subcarriers with a given $\theta = 0.01$ and with different scaled circuit powers P_{C_R} . With spectral-efficient power allocation, the effective capacity increases with increasing $\overline{P^R}$. However, the energy-efficient power allocation achieves the same EC until a given break-point, where the EC flattens out and saturates afterwards. This is due to the fact that, after the breakpoint $\overline{P_{\text{un}}^*}$, increasing power does not benefit EE, and thus, as shown in Section III-C for any $\overline{P^R} \geq$

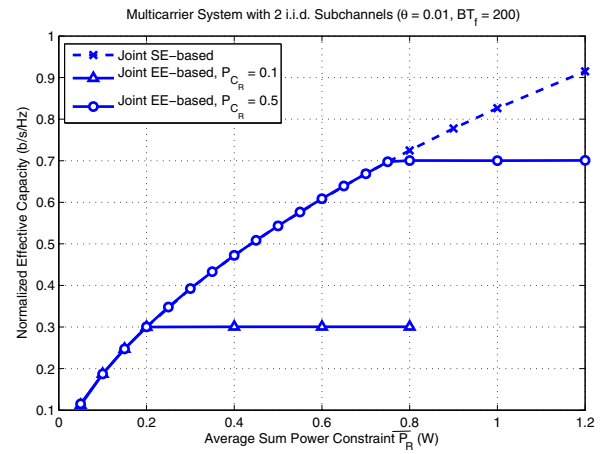


Fig. 9: EC versus average power constraint for multicarrier system with 2 subcarriers.

$\overline{P_{\text{un}}^*}$, the proposed jointly optimal EE allocation does not use all the available power but rather operates at a fixed power level of $\overline{P_{\text{un}}^*}$ and in turn, achieves a certain EC.

Figure 10 shows the maximum achievable QoS-driven EE versus the scaled sum power constraint $\overline{P^R}$ for the same system. Similarly, with energy-efficient power allocation, the maximum achievable QoS-driven EE increases with increasing $\overline{P^R}$ until a given break-point where the QoS-driven EE saturates. Again, the reason is that the proposed jointly optimal allocation operates at the global optimal power level $\overline{P_{\text{un}}^*}$ for any $\overline{P^R} \geq \overline{P_{\text{un}}^*}$. On the other hand, with a spectral-efficient power allocation, the QoS-driven EE decreases after it reaches its maximum. In other words, on the right hand side of the break-point where $\overline{P^R}$ is relatively high, the proposed EE-based power allocation maintains EE by sacrificing SE. However, on the left hand side of the break-point where $\overline{P^R}$ is relatively low, we do not trade off SE for EE. Furthermore, with energy-efficient power allocation, the figures also reveal that increasing P_{C_R} decreases the QoS-driven EE and shifts the break-point to the right such that the EC is increased beyond the break-point. The results indicate that the proposed energy-efficient scheme is more fruitful at low values of P_{C_R} where the EE gains are more pronounced.

V. CONCLUSIONS

We considered the problem of energy-efficient power allocation for multicarrier systems where the receiver requires a target delay-outage probability for its successful communication. We showed that the optimal QoS-driven EE can be achieved through fractional programming. First, we proved that the EE is quasi-concave in the subcarrier power allocations. Next, we solved the EE optimization problem without considering any input transmit power constraint. We showed that the unconstrained optimal EE could be obtained using a two-step algorithm by first finding the optimum average sum power level and then distributing the subcarrier powers optimally over both frequency and time based on this level using a traditional SE-based allocation. In contrary to delay-unconstrained system, the structure of the QoS-driven EE-optimal power allocation is not a standard water-filling approach, but rather depends

$$\begin{aligned} \frac{\partial^2 f(\mathbf{P}^R)}{\partial P_i^{R2}} &= \frac{\Lambda''(\mathbf{P}^R)\Lambda(\mathbf{P}^R) - (\Lambda'(\mathbf{P}^R))^2}{\Lambda^2(\mathbf{P}^R)} \\ &= \frac{\beta(\beta+1)\mathbb{E}_{\mathbf{x}}\left[\frac{x_i^2}{(1+P_i^R x_i)^2}\prod_{n=1}^N U_n\right]\mathbb{E}_{\mathbf{x}}\left[\prod_{n=1}^N U_n\right] - \beta^2\left(\mathbb{E}_{\mathbf{x}}\left[\frac{x_i}{1+P_i^R x_i}\prod_{n=1}^N U_n\right]\right)^2}{\left(\mathbb{E}_{\mathbf{x}}\left[\prod_{n=1}^N U_n\right]\right)^2}, \end{aligned} \quad (27a)$$

$$\begin{aligned} \frac{\partial^2 f(\mathbf{P}^R)}{\partial P_i^R \partial P_j^R} &= \frac{G'(\mathbf{P}^R)\Lambda(\mathbf{P}^R) - \Lambda'(\mathbf{P}^R)G(\mathbf{P}^R)}{\Lambda^2(\mathbf{P}^R)}, \quad \forall i \neq j, \\ &= \frac{\beta^2\mathbb{E}_{\mathbf{x}}\left[\frac{x_i x_j}{(1+P_i^R x_i)(1+P_j^R x_j)}\prod_{n=1}^N U_n\right]\mathbb{E}_{\mathbf{x}}\left[\prod_{n=1}^N U_n\right] - \beta^2\mathbb{E}_{\mathbf{x}}\left[\frac{x_i}{1+P_i^R x_i}\prod_{n=1}^N U_n\right]\mathbb{E}_{\mathbf{x}}\left[\frac{x_j}{1+P_j^R x_j}\prod_{n=1}^N U_n\right]}{\left(\mathbb{E}_{\mathbf{x}}\left[\prod_{n=1}^N U_n\right]\right)^2}, \end{aligned} \quad (27b)$$

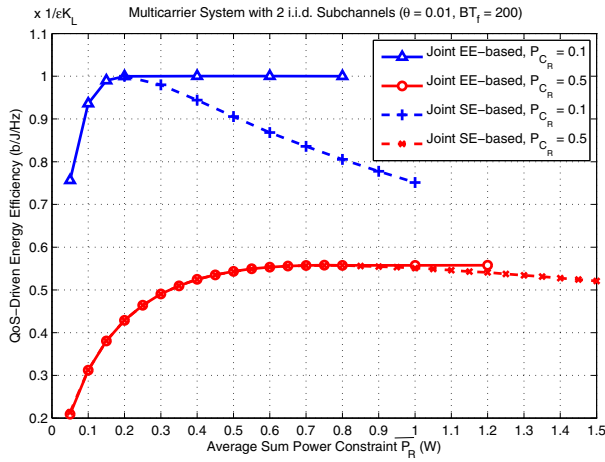


Fig. 10: EE versus average power constraint for multicarrier system with 2 subcarriers.

on both the circuit power as well as the delay requirement. Having solved the power-unconstrained problem, a total power constraint is introduced and the solution is now developed under an average sum transmit power constraint. Numerical results demonstrate significant EE gains over the independent subcarrier optimization approach with more pronounced gains in systems with more stringent delay constraints, as well as in fading channels with higher frequency selectivity. Further, the buffer size required for achieving a specific delay-outage probability is characterized for any given operating throughput. The effect of the transmit power constraint on the rate-energy tradeoff has been analyzed wherein the proposed EE-based power allocation maximizes EE by sacrificing SE at values of \bar{P}^R greater than a certain threshold, while the EC is maintained at values of \bar{P}^R lower than that threshold. The threshold was shown to be an increasing function of the circuit power consumption.

APPENDIX A

PROOF OF THEOREM 1

Let $f(\mathbf{P}^R)$ be a function of the power allocations $\{P_n^R \geq 0, n = 1, 2, \dots, N\}$ as

$$f(\mathbf{P}^R) = \ln(\Lambda(\mathbf{P}^R)), \quad (25)$$

where $\Lambda(\mathbf{P}^R) = \mathbb{E}_{\mathbf{x}}\left[\prod_{n=1}^N U_n(x_n, P_n^R)\right]$ and $U_n(x_n, P_n^R) = (1 + x_n P_n^R(\theta, \gamma))^{-\beta} > 0$. Taking $U_n(x_n, P_n^R)$ as U_n for simplicity, the first partial derivative of $f(\mathbf{P}^R)$ with respect to $P_i^R, \forall i = 1, 2, \dots, N$, is found to be always negative as

$$\begin{aligned} \frac{\partial f(\mathbf{P}^R)}{\partial P_i^R} &= \frac{\Lambda'(\mathbf{P}^R)}{\Lambda(\mathbf{P}^R)} \\ &= \frac{-\beta \cdot \mathbb{E}_{\mathbf{x}}\left[\frac{x_i}{1+P_i^R x_i}\prod_{n=1}^N U_n\right]}{\mathbb{E}_{\mathbf{x}}\left[\prod_{n=1}^N U_n\right]} < 0, \end{aligned} \quad (26)$$

where $\Lambda'(\mathbf{P}^R)$ is the first partial derivative of $\Lambda(\mathbf{P}^R)$ with respect to P_i^R . In turn, the second partial derivatives can be obtained as in (27a) and (27b) (which can be found at the top of the previous page), where $G(\mathbf{P}^R)$ is the first partial derivative of $\Lambda(\mathbf{P}^R)$ with respect to P_j^R and $G'(\mathbf{P}^R) = \frac{\partial G}{\partial P_i^R} = \frac{\partial^2 \Lambda(\mathbf{P}^R)}{\partial P_i^R \partial P_j^R} = \frac{\partial^2 \Lambda(\mathbf{P}^R)}{\partial P_j^R \partial P_i^R}$. In order to have unique notations for the different higher-order derivatives, the superscript primes are solely dedicated for differentiation with respect to P_i^R .

Since $\{x_i, \forall i = 1, \dots, N\}$ are i.i.d. random variables such that $\mathbb{E}[h(x_i)] = \mathbb{E}[h(x_j)] \forall i, j = 1, \dots, N$ for any function $h(\cdot)$, then the partial derivative $b \equiv \frac{\partial^2 f(\mathbf{P}^R)}{\partial P_i^{R2}}$ is constant $\forall i = 1, 2, \dots, N$, whereas the partial derivative $a \equiv \frac{\partial^2 f(\mathbf{P}^R)}{\partial P_i^R \partial P_j^R}$ is also constant $\forall i \neq j$. Thus, the Hessian of the function $f(\mathbf{P}^R)$ is

$$\begin{aligned}
 \Psi(\mathbf{P}^R) &= \Lambda''(\mathbf{P}^R)\Lambda(\mathbf{P}^R) - (\Lambda'(\mathbf{P}^R))^2 + (N-1) [G'(\mathbf{P}^R)\Lambda(\mathbf{P}^R) - \Lambda'(\mathbf{P}^R)G(\mathbf{P}^R)] \\
 &= \beta(\beta+1)\mathbb{E}_{\mathbf{x}} \left[\frac{x_i^2}{(1+P_i^R x_i)^2} \prod_{n=1}^N U_n \right] \mathbb{E}_{\mathbf{x}} \left[\prod_{n=1}^N U_n \right] + (N-1)\beta^2 \mathbb{E}_{\mathbf{x}} \left[\frac{x_i x_j}{(1+P_i^R x_i)(1+P_j^R x_j)} \prod_{n=1}^N U_n \right] \mathbb{E}_{\mathbf{x}} \left[\prod_{n=1}^N U_n \right] \\
 &\quad - N\beta^2 \left(\mathbb{E}_{\mathbf{x}} \left[\frac{x_i}{1+P_i^R x_i} \prod_{n=1}^N U_n \right] \right)^2. \tag{32}
 \end{aligned}$$

an $N \times N$ real symmetric matrix given by

$$\nabla^2 f(\mathbf{P}^R) = \begin{bmatrix} b & a & \dots & a \\ a & b & & \vdots \\ \vdots & & \ddots & a \\ a & \dots & a & b \end{bmatrix}_{N \times N}. \tag{28}$$

Hence, using real Schur decomposition, the Hessian in (28) can be decomposed as

$$\nabla^2 f(\mathbf{P}^R) = \mathbf{V} \begin{bmatrix} b+(N-1)a & 0 & \dots & 0 \\ 0 & b-a & & \vdots \\ \vdots & & \ddots & 0 \\ 0 & \dots & 0 & b-a \end{bmatrix} \mathbf{V}^T,$$

where \mathbf{V} is an orthogonal matrix and the entries of the diagonal matrix, $b-a$ and $b+(N-1)a$, are the eigenvalues of $\nabla^2 f(\mathbf{P}^R)$.

APPENDIX B

PROOF OF THEOREM 2

Based on Theorem 1, $\nabla^2 f(\mathbf{P}^R)$ has two distinct eigenvalues. First, we investigate whether the eigenvalue $\lambda_1 \equiv b-a$ is positive or not by expressing it as

$$\begin{aligned}
 \lambda_1 &= \frac{1}{\mathbb{E}_{\mathbf{x}} \left[\prod_{n=1}^N U_n \right]} \left(\beta(\beta+1)\mathbb{E}_{\mathbf{x}} \left[\frac{x_i^2}{(1+P_i^R x_i)^2} \prod_{n=1}^N U_n \right] \right. \\
 &\quad \left. - \beta^2 \mathbb{E}_{\mathbf{x}} \left[\frac{x_i x_j}{(1+P_i^R x_i)(1+P_j^R x_j)} \prod_{n=1}^N U_n \right] \right). \tag{29}
 \end{aligned}$$

Since $\beta \cdot \mathbb{E}_{\mathbf{x}} \left[\frac{x_i^2}{(1+P_i^R x_i)^2} \prod_{n=1}^N U_n \right] > 0$, it can be easily seen from (29) that

$$\begin{aligned}
 \lambda_1 > \Omega &\equiv \frac{\beta^2}{\mathbb{E}_{\mathbf{x}} \left[\prod_{n=1}^N U_n \right]} \left(\mathbb{E}_{\mathbf{x}} \left[\frac{x_i^2}{(1+P_i^R x_i)^2} \prod_{n=1}^N U_n \right] \right. \\
 &\quad \left. - \mathbb{E}_{\mathbf{x}} \left[\frac{x_i x_j}{(1+P_i^R x_i)(1+P_j^R x_j)} \prod_{n=1}^N U_n \right] \right). \tag{30}
 \end{aligned}$$

Due to the i.i.d. property of $\{x_i, \forall i = 1, \dots, N\}$, we further note that

$$\begin{aligned}
 2\Omega &= \frac{\beta^2}{\mathbb{E}_{\mathbf{x}} \left[\prod_{n=1}^N U_n \right]} \left(\mathbb{E}_{\mathbf{x}} \left[\left(\frac{x_i^2}{(1+P_i^R x_i)^2} + \frac{x_j^2}{(1+P_j^R x_j)^2} \right. \right. \right. \\
 &\quad \left. \left. - \frac{2x_i x_j}{(1+P_i^R x_i)(1+P_j^R x_j)} \right) \prod_{n=1}^N U_n \right] \right) \\
 &= \frac{\beta^2 \mathbb{E}_{\mathbf{x}} \left[\left(\frac{x_i}{1+P_i^R x_i} - \frac{x_j}{1+P_j^R x_j} \right)^2 \prod_{n=1}^N U_n \right]}{\mathbb{E}_{\mathbf{x}} \left[\prod_{n=1}^N U_n \right]} > 0. \tag{31}
 \end{aligned}$$

Since $\Omega > 0$ and $\lambda_1 > \Omega$, then λ_1 must also be positive.

Now, let investigate whether the remaining eigenvalue $\lambda_2 \equiv b+(N-1)a$ is also positive. Since the denominator of λ_2 is always positive from (27a) and (27b), it is sufficient to prove that the numerator is positive. Denoting the numerator of λ_2 by $\Psi(\mathbf{P}^R)$, we get (32) (which can be found at the top of the next page).

The value for $\Psi(\mathbf{P}^R)$ at $\mathbf{P}^R = \mathbf{0}$ and $\mathbf{P}^R \rightarrow \infty$ can be obtained and bounded using the Jensen's inequality as

$$\Psi(\mathbf{P}^R) |_{\mathbf{P}^R=\mathbf{0}} = \beta(\beta+1)\mathbb{E}_{\mathbf{x}} [x_i^2] - \beta^2 \mathbb{E}_{\mathbf{x}} [x_i]^2 \geq 0, \tag{33a}$$

$$\Psi(\mathbf{P}^R) |_{\mathbf{P}^R \rightarrow \infty} \rightarrow 0. \tag{33b}$$

We now prove by contradiction that $\Psi(\mathbf{P}^R)$ can never cross the zero axis. Assume that $\Psi(\mathbf{P}^R)$ crosses the zero axis.

First, we show that the function $\chi(\mathbf{P}^R) = N \frac{\partial f(\mathbf{P}^R)}{\partial P_i^R}$ whose derivative is λ_2 , i.e., $\lambda_2 = \frac{\partial \chi(\mathbf{P}^R)}{\partial P_i^R}$, is always negative since

$$N \frac{\partial f(\mathbf{P}^R)}{\partial P_i^R} = \frac{\partial f(\mathbf{P}^R)}{\partial P_i^R} + (N-1) \frac{\partial f(\mathbf{P}^R)}{\partial P_j^R} < 0. \tag{34}$$

Using (26), we further note that

$$\frac{\partial \chi(\mathbf{P}^R)}{\partial P_i^R} \Big|_{\mathbf{P}^R \rightarrow \infty} \rightarrow 0. \tag{35}$$

Then, due to (35) and the fact that λ_2 is a continuous increasing function at $\mathbf{P}^R = \mathbf{0}$, it can be shown that $\Psi(\mathbf{P}^R)$ has to cross the zero axis at least twice. Since $\Psi(\mathbf{P}^R)$ is a continuous function, then it must have a stationary point between the two points where it crosses the zero axis. Consequently, due to (33b), $\Psi(\mathbf{P}^R)$ will have another stationary point after it crosses the zero axis for the second time. Hence, $\Psi'(\mathbf{P}^R)$ has

to also cross the zero axis twice. Similarly for any n , since $\Psi^{(n)}(\mathbf{P}^R) = \frac{\partial^n \Psi(\mathbf{P}^R)}{\partial (\mathbf{P}^R)^n}$ is a continuous function that tends to zero when $\mathbf{P}^R \rightarrow \infty$, then recursively $\Psi^{(n)}(\mathbf{P}^R)|_{n \rightarrow \infty}$ has to cross the zero axis twice.

On another side, we note that the n^{th} derivative of $\Psi(\mathbf{P}^R)$ can be determined from (32) as

$$\begin{aligned} \Psi^{(n)}(\mathbf{P}^R) &= \Lambda^{(n+2)}(\mathbf{P}^R) \Lambda(\mathbf{P}^R) \\ &+ \Lambda^{(n+1)}(\mathbf{P}^R) \left(c_{11} \Lambda'(\mathbf{P}^R) + c_{12} G'(\mathbf{P}^R) \right) \\ &+ \Lambda^{(n)}(\mathbf{P}^R) \left(c_{21} \Lambda''(\mathbf{P}^R) + c_{22} G''(\mathbf{P}^R) \right) + \dots, \end{aligned} \quad (36)$$

with constants $\{c_{mn}\}$ such that

$$\begin{aligned} &\frac{\Lambda^{(n+1)}(\mathbf{P}^R) \left(c_{11} \Lambda'(\mathbf{P}^R) + c_{12} G'(\mathbf{P}^R) \right)}{\Lambda^{(n+2)}(\mathbf{P}^R) \Lambda(\mathbf{P}^R)} \Big|_{n \rightarrow \infty} \\ &= c \cdot \frac{\prod_{k=1}^{n+1} (\beta + k - 1) \mathbb{E}_x \left[\left(\frac{x_i}{1 + P_i^R x_i} \right)^{n+1} \prod_{n=1}^N U_n \right]}{\prod_{k=1}^{n+2} (\beta + k - 1) \mathbb{E}_x \left[\left(\frac{x_i}{1 + P_i^R x_i} \right)^{n+2} \prod_{n=1}^N U_n \right]} \Big|_{n \rightarrow \infty} \\ &= 0, \end{aligned} \quad (37)$$

where c is a constant that does not depend on n . In the view of (37), the same behavior is maintained for the remaining terms of the series in (36), and therefore, $\Psi^{(n)}(\mathbf{P}^R)|_{n \rightarrow \infty} = \Lambda^{(n+2)}(\mathbf{P}^R) \Lambda(\mathbf{P}^R)|_{n \rightarrow \infty}$ cannot be zero. Hence, by contradiction, we can conclude that the initial assumption must be false and, as such, $\Psi(\mathbf{P}^R)$ never crosses the zero axis. Since $\Psi(\mathbf{P}^R)|_{\mathbf{P}^R=0}$ is found to be positive, then $\Psi(\mathbf{P}^R)$ is always positive. As a result, all the eigenvalues of the Hessian function of $f(\mathbf{P}^R)$ are positive and, in turn, $\nabla^2 f(\mathbf{P}^R)$ is positive semi-definite.

APPENDIX C

PROOF OF THEOREM 3

Since the EE objective function, $EE(\theta)$, in (12) is shown to be a ratio of a concave to a non-negative affine function in $\mathbf{P}^R(\theta, \gamma)$, then $EE(\theta)$ is a quasi-concave function of the subcarrier power allocations. In other words, the sublevel sets of $EE(\theta)$ is strictly convex for any real ξ and can be given as

$$S_\xi = \{ \mathbf{P}^R(\theta, \gamma) \succeq \mathbf{0} | EE(\theta) \geq \xi \}, \quad (38)$$

where \succeq denotes vector inequality and hence, $\mathbf{P}^R(\theta, \gamma) \succeq \mathbf{0}$ indicates that each element of $\mathbf{P}^R(\theta, \gamma)$ is non-negative. Strictly quasi-concave functions are unimodal such that every local maximum is a unique global one. Denote this unique global maximum by $\overline{P}_{\text{un}}^*$, which is essentially the average sum power at which the unconstrained EE in (12) is maximized. Therefore, $EE(\theta)$ is an increasing function of average power until $\overline{P}_{\text{un}}^*$, beyond which the EE decreases with power.

Applying a constraint on the average sum transmit power \overline{P}^R , it can be easily seen that the optimal solution to the constrained problem in (23) is either the global solution of the problem or the boundary at which the constraint intersects the QoS-driven EE function. In the case where $\overline{P}^R < \overline{P}_{\text{un}}^*$, the maximum EE, $EE^{\text{opt}}(\theta)$, is achieved at \overline{P}^R since $EE(\theta)$ is increasing till \overline{P}^R . Accordingly, the optimum value for

the denominator of $EE^{\text{opt}}(\theta)$ is now fixed to $P_{C_R} + \overline{P}^R$. In conclusion, the QoS-driven EE maximization reduces to maximizing the EC with an average input power limit set to \overline{P}^R .

REFERENCES

- [1] C.-S. Chang, "Stability, queue length, and delay of deterministic and stochastic queueing networks," *IEEE Trans. Automat. Contr.*, vol. 39, no. 5, pp. 913–931, May 1994.
- [2] D. Wu and R. Negi, "Effective capacity: a wireless link model for support of quality of service," *IEEE Trans. Wireless Commun.*, vol. 2, no. 4, pp. 630–643, July 2003.
- [3] J. Tang and X. Zhang, "Quality-of-service driven power and rate adaptation for multichannel communications over wireless links," *IEEE Trans. Wireless Commun.*, vol. 6, no. 12, pp. 4349–4360, Dec. 2007.
- [4] —, "Quality-of-service driven power and rate adaptation over wireless links," *IEEE Trans. Wireless Commun.*, vol. 6, no. 8, pp. 3058–3068, Aug. 2007.
- [5] S. Verdú, "Spectral efficiency in the wideband regime," *IEEE Trans. Inf. Theory*, vol. 48, no. 6, pp. 1319–1343, June 2002.
- [6] G. Li, Z. Xu, C. Xiong, C. Yang, S. Zhang, Y. Chen, and S. Xu, "Energy-efficient wireless communications: tutorial, survey, and open issues," *IEEE Trans. Wireless Commun.*, vol. 18, no. 6, pp. 28–35, Dec. 2011.
- [7] G. Miao, N. Himayat, Y. Li, and D. Bormann, "Energy efficient design in wireless OFDMA," in *Proc. 2008 IEEE Int. Conf. Commun.*, pp. 3307–3312.
- [8] G. Miao, N. Himayat, and G. Li, "Energy-efficient link adaptation in frequency-selective channels," *IEEE Trans. Commun.*, vol. 58, no. 2, pp. 545–554, Feb. 2010.
- [9] C. Isheden and G. Fettweis, "Energy-efficient multi-carrier link adaptation with sum rate-dependent circuit power," in *Proc. 2010 IEEE Global Telecommun. Conf.*, pp. 1–6.
- [10] —, "Energy-efficient link adaptation on a Rayleigh fading channel with receiver CSI," in *Proc. 2011 IEEE Int. Conf. Commun.*, pp. 1–5.
- [11] —, "Energy-efficient link adaptation with transmitter CSI," in *Proc. 2011 IEEE Wireless Commun. Netw. Conf.*, pp. 1381–1386.
- [12] M. Gursoy, D. Qiao, and S. Velipasalar, "Analysis of energy efficiency in fading channels under QoS constraints," *IEEE Trans. Wireless Commun.*, vol. 8, no. 8, pp. 4252–4263, Aug. 2009.
- [13] D. Qiao, M. Gursoy, and S. Velipasalar, "Energy efficiency in the low-SNR regime under queueing constraints and channel uncertainty," *IEEE Trans. Commun.*, vol. 59, no. 7, pp. 2006–2017, July 2011.
- [14] L. Musavian and T. Le-Ngoc, "Energy-efficient power allocation for delay-constrained systems," in *Proc. 2012 IEEE Global Commun. Conf.*
- [15] C. Isheden, Z. Chong, E. Jorswieck, and G. Fettweis, "Framework for link-level energy efficiency optimization with informed transmitter," *IEEE Trans. Wireless Commun.*, vol. 11, no. 8, pp. 2946–2957, Aug. 2012.



Amir Helmy (S'12) received the B.Eng. degree (Hons) in electrical engineering from McGill University, Montréal, QC, Canada, in 2011. He is currently finishing the M.Eng. degree (thesis) in electrical engineering at McGill University.

From September 2009 to June 2010, he was an Intern (Co-op) with InterDigital Canada Ltée, Montréal, where he worked on research and development of cellular system evolution, as part of the Long Term Evolution team. His research interests include digital communications and dynamic resource management for wireless networks, with emphasis on cooperative communications, quality-of-service provisioning and energy efficiency.

Mr. Helmy received the 2012 Alexander Graham Bell Canada Graduate Scholarship from the National Sciences and Engineering Research Council of Canada.



Leila Musavian (S'05-M'07) received the Ph.D. degree in Telecommunications from Kings College London, U.K., in 2006. She is currently working as a lecturer in communications in the School of Computing and Communications, InfoLab21, Lancaster University. Prior to that (2010-2012), she was a Research Associate in the Department of Electrical and Computer Engineering, McGill University, and was working on developing energy-efficient resource allocation techniques for multi-user wireless communications systems. Between 2009 and 2010, she

was with Loughborough University and investigated adaptive transmission techniques for delay Quality-of-Service (QoS) provisioning in Cognitive Radio Networks (CRNs). She was a post-doctoral fellow at National Institute of Scientific Research-Energy, Materials, and Telecommunications (INRS-EMT), University of Quebec, Canada, from 2006 to 2008. Her research interests lie in the area of wireless communications and include radio resource management for next generation wireless networks, CRNs, green communication and energy-efficient transmission techniques, cross-layer design for delay QoS provisioning in spectrum-sharing channels.



Tho Le-Ngoc (F'97) received the B.Eng. degree (with Distinction) in Electrical Engineering and the M.Eng. degree from McGill University, Montréal, QC, Canada, in 1976 and 1978, respectively, and the Ph.D. degree in Digital Communications from the University of Ottawa, Ottawa, ON, Canada, in 1983.

During 1977-1982, he was with Spar Aerospace Limited, Montréal, QC, Canada, engaged in the development and design of satellite communications systems. During 1982-1985, he was an Engineering Manager of the Radio Group with the Department of

Development Engineering, SRTelecom Inc., Montréal, where he developed the new point-to-multipoint DA-TDMA/TDM Subscriber Radio System SR500. During 1985-2000, he was a Professor with the Department of Electrical and Computer Engineering, Concordia University, Montréal. Since 2000, he has been with the Department of Electrical and Computer Engineering, McGill University. His research interest includes broadband digital communications.

Dr. Le-Ngoc is a Fellow of the Institute of Electrical and Electronics Engineers (IEEE), the Engineering Institute of Canada (EIC), the Canadian Academy of Engineering (CAE) and the Royal Society of Canada (RSC). He is the recipient of the 2004 Canadian Award in Telecommunications Research, and recipient of the IEEE Canada Fessenden Award 2005. He holds a Canada Research Chair (Tier I) in Broadband Access Communications and a Bell Canada/Natural Sciences and Engineering Research Council of Canada Industrial Research Chair in Performance and Resource Management in Broadband xDSL Access Networks.